SCIENCE CHINA
Earth Sciences

•RESEARCH PAPER•

January 2023 Vol.66 No.1: 111–128
https://doi.org/10.1007/s11430-021-9988-5

Spatially explicit reconstruction of cropland cover for China over the past millennium

Fanneng HE[1], Fan YANG[2*], Caishan ZHAO[1,3], Shicheng LI[4] & Meijiao LI[5]

[1] *Key Laboratory of Land Surface Pattern and Simulation, Institute of Geographic Sciences and Natural Resources Research, Chinese Academy of Sciences, Beijing 100101, China;*
[2] *Key Research Institute of Yellow River Civilization and Sustainable Development & Collaborative Innovation Center on Yellow River Civilization Jointly Built By Henan Province and Ministry of Education, Henan University, Kaifeng 475001, China;*
[3] *University of Chinese Academy of Sciences, Beijing 100049, China;*
[4] *School of Public Administration, China University of Geosciences, Wuhan 430074, China;*
[5] *College of Resources and Environment, Shanxi University of Finance and Economics, Taiyuan 030006, China*

Received July 15, 2021; revised June 7, 2022; accepted August 10, 2022; published online November 10, 2022

Abstract Reconstructing historical land use and land cover change using explicit temporal, quantitative, and spatial information is not only the prerequisite for simulating long-term climate change and ecological effects but is also a scientific basis for comprehensively understanding the process and mechanism of anthropogenic land use alterations. Considering changes in historical borders and administrative divisions, a provincial cropland area dataset for China over the past millennium was created on the basis of existing estimations since the Song Dynasty. Land suitability for cultivation was then assessed by incorporating altitude, slope, soil texture, and the maximum potential productivity of climate. Subsequently, a gridding allocation model for cropland was constructed, and the provincial cropland area for 24 years over the past millennium was allocated into grids with a resolution of 10 km. The cropland area in China increased from 3.71×10^7 ha in AD 1000 to 12.92×10^7 ha in AD 1999, with a peak of 13.50×10^7 ha in AD 1980. The total cropland area in China showed fluctuating increasing trends that can be divided into three phases: fluctuation without notable net change for AD 1000–1290, slow increase for AD 1290–1661, and rapid increase for AD 1661–1999. Spatially, cropland intensified in the middle-lower reaches of the Yellow and Yangtze Rivers and expanded to mountainous and frontier areas over the last millennium. Specifically, over the entire period, the fractional cropland areas (FCAs) in the middle-lower reaches of the Yellow and Yangtze Rivers increased by 1.4 and 0.8 times, respectively. Since the mid-Qing Dynasty, large-scale land reclamation expanded to areas of low reclamation in southwest and northeast China. The FCAs for southwest and northeast China increased from 2.13% and 0.55% in AD 1661 to 18.00% and 26.61% in AD 1999, respectively. For AD 1661–1999, the proportion of cropland increased by 55% in the hills and low mountains and 27% in the middle and high mountains. The comparison with remote sensing cropland data shows that the grid cells with absolute differences of 0–10% accounted for 70.35% of all grid cells, while grids with differences exceeding 60% accounted for only 0.83%. This finding indicates that the reconstruction method is feasible, and the reconstruction results objectively reveal the historical spatiotemporal changes in cropland.

Keywords Land use and land cover change, Historical cropland, Gridding reconstruction, China, Last millennium

Citation: He F, Yang F, Zhao C, Li S, Li M. 2023. Spatially explicit reconstruction of cropland cover for China over the past millennium. Science China Earth Sciences, 66(1): 111–128, https://doi.org/10.1007/s11430-021-9988-5

* Corresponding author (email: yangfan@henu.edu.cn)

1. Introduction

Human land use activities over long periods have substantially altered the landscape of the Earth's surface (Ellis et al., 2013; Verburg et al., 2015; Stephens et al., 2019) and profoundly affected climate and terrestrial ecosystems at regional and global scales (Scott et al., 2018; Nikiel and Eltahir, 2019; Mendelsohn and Sohngen, 2019). The reconstruction of historical land use and land cover change (LUCC) using explicit temporal, quantitative, and spatial information is vital for understanding past global change, modeling long-term climate change, carbon emissions, and the ecological effects of human activities.

Therefore, many global projects, including PAGES (Past Global Changes) and GLP (Global Land Project), made considerable efforts to reconstruct historical LUCC from local to global scales, resulting in several well-known global historical land use datasets, including anthropogenic land use estimates dataset for the Holocene (HYDE) (Klein Goldewijk et al., 2011, 2017), the preindustrial land cover change scenario (KK10) (Kaplan et al., 2009, 2011), the global LUCC dataset for the last millennium (PJ) (Pongratz et al., 2008), and the cropland and pasture dataset from AD 1700 to 2007 (SAGE) (Ramankutty and Foley, 1999; Ramankutty et al., 2012). These datasets provide important primary data for modeling long-term global climate change. However, these global datasets should be carefully applied at regional and local scales (Ramankutty and Foley, 1999). For instance, the cropland estimates for Europe and Brazil in the global datasets (SAGE and HYDE 3.1) are lower than those from regional studies (Leite et al., 2012; Kaplan et al., 2017). Several deviations appear in the spatial patterns despite the highly consistent total cropland areas for Germany in HYDE 3.2 with studies based on region-specific sources (Zhang et al., 2021). Evaluations of long-term cropland data in China also indicate that the reconstructions of HYDE and KK10 are highly uncertain and do not capture historical land use facts and processes in China (Li et al., 2010; He et al., 2013; Li et al., 2019; Fang et al., 2020).

Many long-term regional LUCC datasets, including the conterminous US cropland areas for AD 1850–2000 (Zumkehr and Campbell, 2013), the Europe LUCC data for AD 1900–2010 (Fuchs et al., 2013, 2015), the India land use dataset for AD 1880–2010 (Tian et al., 2014), and the Brazil land use data for AD 1940–1995 (Leite et al., 2012), have been reconstructed on the basis of region-specific historical archives to provide reliable historical LUCC data considering regional studies and improve global datasets. China has a long history of land reclamation and abundant historical documents. Based on these historical documents, significant progress has been made in the reconstruction of historical cropland areas on national and regional scales (Ge et al., 2004; Ye et al., 2009; Yang et al., 2015, 2021; Li et al., 2016; He et al., 2017; Guo et al., 2021). These studies have provided primary data to simulate climate change and estimates the carbon budget of Chinese terrestrial ecosystems (Ge et al., 2008; Li et al., 2014; Yang et al., 2019). However, most gridding cropland reconstructions only focused on the last 300 years (He et al., 2019), and only a few scholars estimated the cropland areas over the last millennium (He et al., 2017; Li et al., 2018a, 2020), preventing a complete understanding of long-term LUCC in China.

The past millennium has witnessed increasingly prominent ecological problems in China. The spatially explicit reconstructing of the cropland cover for China over the past millennium would provide useful reference data to (1) deepen understanding of the process and mechanism of anthropogenic land use change, (2) reveal the evolution of climate and ecosystem, and (3) predict future scenarios and their impacts. Ten-kilometer cropland cover maps of China from AD 1000 to 1999 were constructed in this study. The reconstruction involved the following four steps. First, based on estimations of cropland areas since the Song (including the Northern and Southern Song), Liao, and Jin Dynasties, provincial cropland areas of present China over the last millennium were obtained by unifying the time slices and spatial ranges. Second, a gridding allocation scheme of historical cropland was established, and the factors affecting the historical cropland distribution were identified. Third, a gridding allocation method for cropland was developed by quantifying the factors closely related to the spatial distribution of cropland. Finally, the provincial cropland area was allocated into grids at a resolution of 10 km using the developed method, and the changes in cropland over the past millennium were analyzed.

2. Data sources and processing

2.1 Data sources

2.1.1 Historical provincial cropland data

Existing provincial cropland area estimations since the Northern Song Dynasty (Table 1) were collected. Using Chinese historical tax records for cropland areas and relevant historical documents, many scholars reconstructed the provincial cropland area for China by analyzing the attributes of various records and devising appropriate reconstruction methods. These reconstruction results can objectively capture historical changes in cropland areas for each period in China.

2.1.2 Historical basic geographical data

The historical population data were obtained from the Population History of China (Vols. 3–6), which includes the years AD 1078, 1102, 1162, 1207, 1223, 1290, 1393, 1630, 1776, 1820, 1910, and 1953 (Wu, 2000; Cao, 2000, 2001;

Table 1 Collection of historical provincial cropland area data for China[a)]

Dynasty	Spatial coverage	Temporal coverage	Reference
Song, Liao, and Jin Dynasties	Northern Song Dynasty: 1 Fu-level unit and 18 Lu-level units Liao Dynasty: five Dao-level units Southern Song Dynasty: 14 Lu-level units Jin Dynasty: 19 Lu-level units	AD 1000, 1066, 1078, 1162, 1215	He et al. (2017); Li et al. (2018b)
Yuan Dynasty	Nine provincial-level units	AD 1290	Li et al. (2018a)
Ming Dynasty	Northern Zhili Province, Southern Zhili Province, 13 provincial-level units, Northeast China (Nurgan and Liaodong)	AD 1393, 1583, 1620	Li et al. (2020)
Qing Dynasty to the present	25 provincial-level units	AD 1661–1999	Ge et al. (2004); Li et al. (2016)
Song Dynasty to the Ming Dynasty	Western China (present-day Xinjiang, Qinghai, and Xizang)	AD 1044, 1151, 1160, 1254, 1268, 1290, 1393	Li et al. (2019)

a) Fu, Lu, and Dao refer to the provincial-level political units in use during each Dynasty.

Hou, 2001). The administrative area and coastline of each dynasty were extracted digitally from the Historical Atlas of China (Tan, 1982) (Figure 1a). The northern farming-pastoral ecotone (FPE) in China over the past millennium was derived from Zou (1995) and Zhang (1996) (Figure 1b). The coastline and FPE data are critical limiting factors of gridding allocation for cropland in eastern China. The historical military-oriented cropland in Xinjiang established by Zhao (2010) and Zhang (2017) was also used in this study to determine the scope of cropland gridding allocation.

2.1.3 Modern basic geographical data

Remotely sensed Chinese 1 km LUCC dataset for AD 1980–2015 (CLUDs, available at http://www.resdc.cn) was used to determine the maximum extent of cropland. This dataset contains six land use/cover types (cropland, forestland, grassland, waterbody, unused land, and built-up land) and 25 subclasses. Data from the following four layers were used to assess land suitability for cultivation (LSC): the altitude layer, which was obtained from the digital elevation model of the Geospatial Data Cloud (http://www.gscloud.cn); the slope layer, which was calculated using the altitude data and ArcGIS software; the layer of maximum potential productivity of climate, which included factors of solar radiation, temperature, humidity, and precipitation, and downloaded from the Data Sharing Infrastructure of Earth System Science (http://www.geodata.cn); the soil texture layer, which included the spatial distribution of sand, silty sand, and clay, was obtained from the Resource and Environment Data Cloud Platform (http://www.resdc.cn).

2.2 Data processing

2.2.1 Selecting the spatial scope and provincial units of the study area

Over the past millennium, China was controlled by the Liao (AD 907–1125), Northern Song (AD 960–1127), Southern Song (AD 1127–1279), Jin (AD 1115–1234), Yuan (AD 1271–1368), Ming (AD 1368–1644), Qing (AD 1644–1912), Republic of China (AD 1912–1949), and the People's Republic of China (AD 1949–present) regimes. Some local regimes and tribal entities existed in the western and northern frontier areas of China, including the Dali (AD 937–1253), Western Xia (AD 1038–1227), Western Liao (AD 1124–1218), and Black Khan (AD 1041–1212) regimes. The borders and administrative divisions of each regime frequently changed over the past millennium. Thus, the spatial scope of present China was used in this study for simplicity, and the present provincial administrative divisions were regrouped into 25 provincial units (Figure 2). Specifically, Gansu and Ningxia were merged into Gan-Ning; Beijing, Tianjin, and Hebei were merged into Jing-Jin-Ji; Shanghai and Jiangsu were merged into Hu-Ning; Fujian and Taiwan were merged into Min-Tai; Guangdong and Hainan were merged into Yue-Qiong; Sichuan and Chongqing were merged into Chuan-Yu.

2.2.2 Adjustment of the provincial cropland area data

The provincial cropland area adjustment involved unifying time slices and spatial ranges.

(1) Unification of the time slices. The available data years of historical document-based provincial cropland were inconsistent, which hindered the establishment of the millennium-scale time series. Therefore, the available years of the datasets covering major agricultural areas in China were set as base years, and the cropland areas of the datasets for other regions were linearly interpolated to these base years by the growth rate of population or cropland area. For instance, the reconstructed cropland areas across eastern China during the Song, Liao, and Jin Dynasties were adjusted into five time slices (i.e., AD 1000, 1066, 1078, 1162, and 1215) based on the population growth rate in the Liao and Jin Dynasties. Similarly, other regions and time slices were adjusted accordingly.

(2) Regrouping of the provincial cropland area. Adminis-

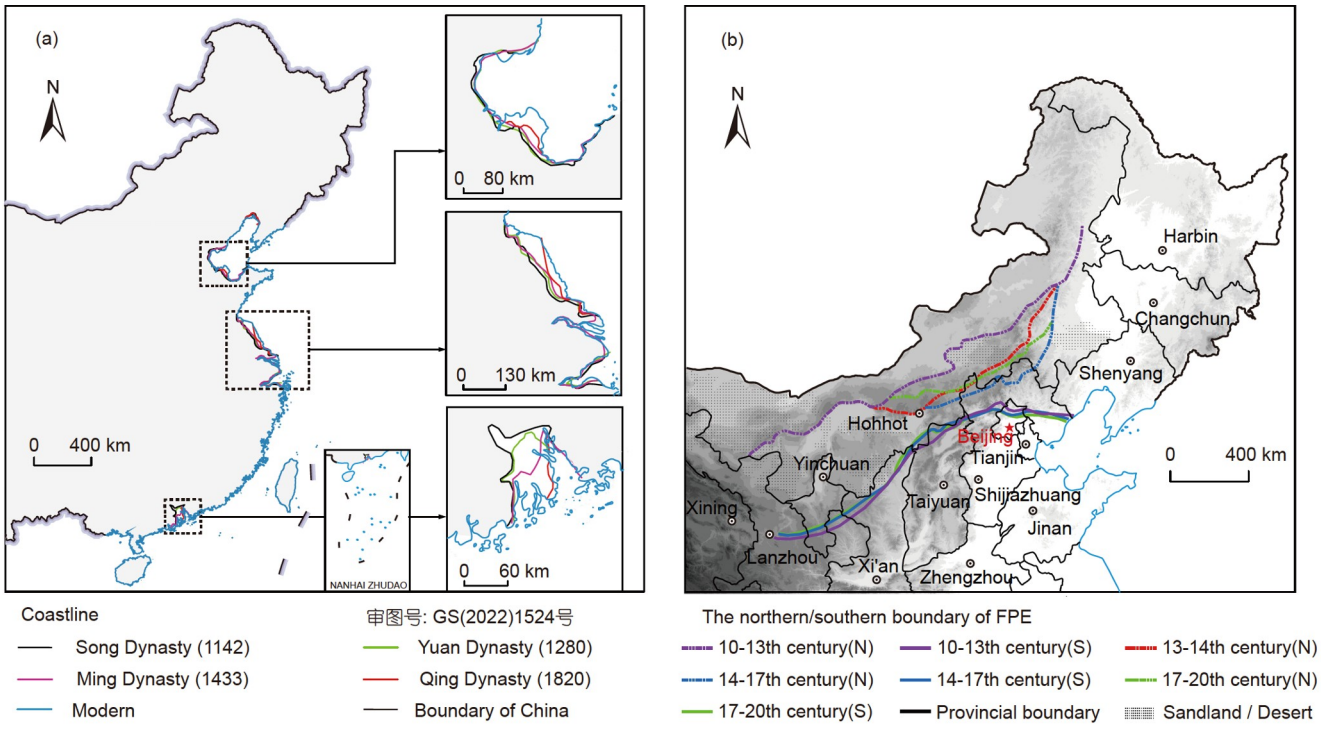

Figure 1 Northern farming-pastoral ecotone (FPE) and coastal zone in China over the past millennium.

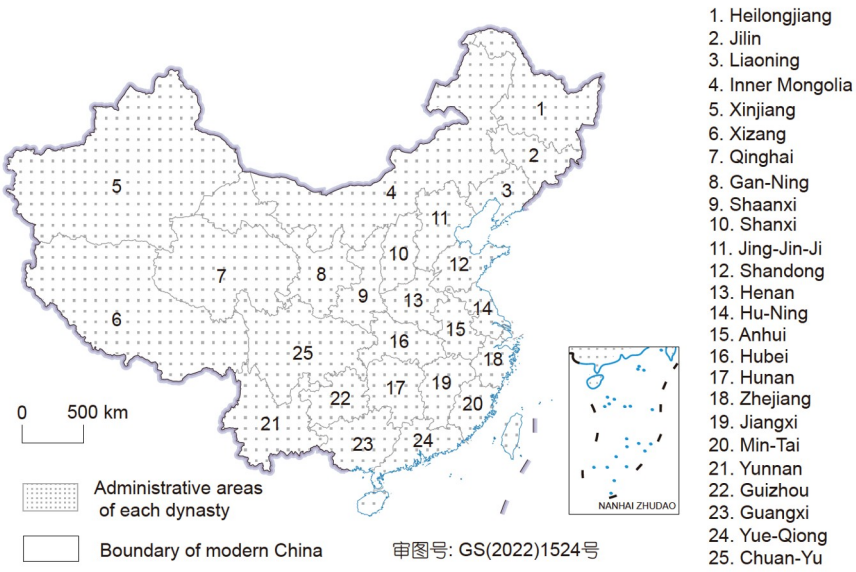

Figure 2 Location, spatial scope, and 25 provincial administrative divisions of China.

trative divisions and their cropland areas in historical periods were merged or split based on the 25 provincial units of Section 2.2.1 to facilitate a consistent analysis. Specifically, three situations are presented. First, when one or more historical provincial administrative divisions are entirely within one of the 25 regrouped provinces, the regrouped provincial cropland area is obtained by merging the original provincial cropland. For instance, Guangnandong Lu of the Northern Song Dynasty and Zhongdu Lu of the Southern Song Dynasty are within the scopes of Yue-Qiong and Jing-Jin-Ji, respectively.

Second, when a historical provincial administrative division is beyond a provincial range of the 25 regrouped provinces and its subprovincial administrative divisions are entirely within a unit of the regrouped provinces, the original provincial cropland areas are first downscaled to subprovincial units by weighting the area and population of the subprovincial units, and the subprovincial cropland areas are

then re-merged to obtain the regrouped provincial cropland. For example, the Jiangzhe Province of the Yuan Dynasty spans three provinces (namely, Hu-Ning, Zhejiang, and Min-Tai), but its subprovincial units (e.g., Jiaxing, Huzhou, Hangzhou, Shaoxing, Qingyuan, Jiande, Wuzhou, Taizhou, Quzhou, Chuzhou, and Wenzhou) are located entirely within the boundaries of these regrouped provinces.

Third, when a historical subprovincial administrative division exceeds the provincial boundaries of the 25 regrouped provinces, the original provincial cropland area was first downscaled to the subprovincial level, and the subprovincial cropland area was then split across the provincial boundaries by weighting its administrative area, slope, and altitude. For example, the Southern Zhili Province of the Ming Dynasty is roughly equivalent to the Hu-Ning and Anhui provinces, and its subprovincial administrative units (Xuzhou, Fengyang, and Huizhou) are beyond the boundary of the two regrouped provinces.

2.2.3 Resampling strategy of spatial resolutions and factor normalization

The target spatial resolution of the gridding cropland dataset was 10 km; therefore, the basic geographical data, including altitude, slope, climate, and soil, were resampled to 10 km. Normalization was performed to characterize the positive relationship between climate and the distribution of cropland (eq. (1)) as well as the negative relationship between terrain (altitude and slope) and the distribution of cropland (eq. (2)).

$$X_{\text{norm}}(i,j)=\frac{X(i,j)}{X_{\max}(i,j)}, \tag{1}$$

$$Y_{\text{norm}}(i,j)=\frac{Y_{\max}(i,j)-Y(i,j)}{Y_{\max}(i,j)}, \tag{2}$$

where $X_{\text{norm}}(i, j)$ and $Y_{\text{norm}}(i, j)$ are normalized climate and terrain factors of grid j in province i, respectively; $X(i, j)$ and $Y(i, j)$ are the values of climate and terrain factors of grid j in province i, respectively; and $X_{\max}(i, j)$ and $Y_{\max}(i, j)$ are the maximum values of climate and terrain factors in province i, respectively.

3. Methods

3.1 Overview of the gridding reconstruction methods

Gridding reconstruction pertains to the allocation of cropland areas into grids based on specific rules. Thus, establishing allocation rules is the core of gridding reconstruction. China boasts a long history of agriculture, and cropland has remained to be an essential resource for the survival and development of the Chinese people. Over the past thousand years, with the continuous increase in population, the area of cropland has continued to rise, and its spatial distribution has also continued to expand overall, especially since the founding of the People's Republic of China. The cropland area has also decreased in some periods. For example, since the 1980s and 1990s, urbanization and the Grain for Green Program have led to a reduction in the cropland area in China, but this reduction accounted for only a small proportion. The aforementioned only decreased by 0.66% from AD 2000 to 2008 (Li et al., 2011) and by 1.73% due to urban land expansion from AD 2000 to 2015 (Yu et al., 2019). These small reductions in cropland area will only slightly impact the overall distribution of cropland. Thus, the distribution of past cropland in China should not exceed the extent of modern cropland.

Subsequently, the core task is to determine the allocation weights of cropland areas at the grid scale. Lands with good natural conditions are always cultivated first based on the history of land cultivation in China. Increasing population pressure and demand for agricultural products lead to the cultivation of marginal lands with high altitudes, large slopes, and low fertility (Wang, 1980; Han, 2012). In other words, the land reclamation process is closely related to the LSC and proceeds from superior land to inferior land (Lin et al., 2009; Yang et al., 2015; Li et al., 2016). Therefore, the allocation weights of cropland areas can be determined by assessing the LSC.

Notably, China has a vast territory with disparate natural environments and social and cultural backgrounds among regions, resulting in different land use practices and agricultural development processes. China is divided into three regions (namely, eastern China, Xinjiang, and Qinghai-Xizang) based on the natural and human environments and the main factors limiting land reclamation to reproduce the spatiotemporal characteristics of land reclamation as objectively as possible (Han, 2012; Li et al., 2015; An et al., 2020). Zoning was then used to reconstruct historical cropland cover.

Overall, after synthesizing the provincial cropland area dataset of China over the past millennium, the subsequent gridding reconstruction for historical cropland cover involved the following steps (Figure 3): (1) determining the maximum extent of cropland distribution based on multiple remote sensing cropland cover data, (2) building an LSC model considering the major factors affecting the spatial distribution of cropland, (3) devising an allocation method for three regions based on factors limiting the cropland cover distribution (including the historical coastlines, northern FPE, and military-oriented cropland in Xinjiang), (4) transforming the provincial cropland area dataset into 10 km cropland cover maps of China for AD1000–1999 by applying the allocation model, and (5) analyzing changes in cropland cover and evaluating the reliability of the proposed reconstruction.

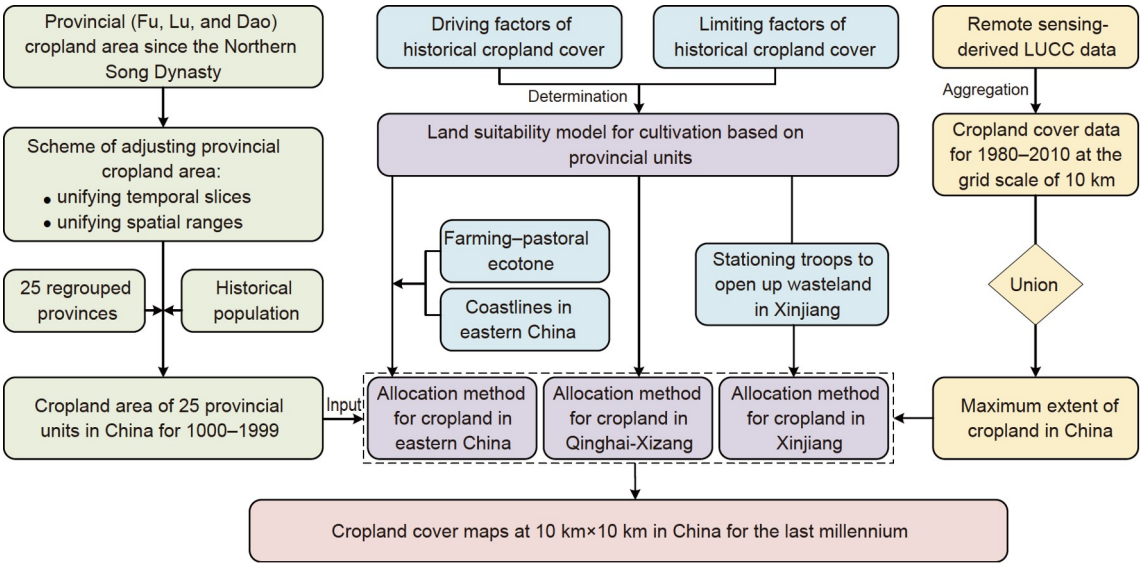

Figure 3 Framework for reconstructing cropland cover in China over the last millennium. Fu, Lu, and Dao refer to the provincial-level political units during each dynasty.

3.2 Gridding allocation method for cropland

3.2.1 Determination of the maximum extent of cropland

Most historical cropland distributions in China should not exceed the extent of modern cropland. Thus, the spatial extents of cropland cover data from the remotely sensed CLUDs for AD 1980, 1990, 2000, and 2010 were merged at a grid scale of 10 km. The synthesized results were regarded as the maximum extent of cropland cover in China (Figure 4).

3.2.2 Land suitability model for cultivation

Land reclamation begins with superior land and then proceeds to inferior land; thus, several factors affecting the spatial distribution of cropland were selected as indexes to assess the LSC. The grid-scale LSC was then determined for each provincial unit.

LSC was determined jointly by the natural environment (e.g., topography, heat, moisture, and soil) and human activities (e.g., agricultural technology, population, and land policy). However, LSC depends on basic land quality and is dominated by natural conditions, and external human factors only restrict the amount of cropland. Replacing historical databases with modern data of the same type is necessary considering their insufficiency. When the area of provincial cropland is known, and the maximum extent of cropland is clear, dominance, stability, and availability of factors affecting the spatial distribution of cropland were taken as gridding allocation principles for cropland. The maximum potential productivity of climate (including light, temperature, and moisture), soil texture, altitude, and slope were selected on the basis of these principles to calculate LSC. The LSC model was constructed with equal weight by normalizing these factors. $L_{\mathrm{suit}}(i,j)$, the LSC value of grid j in province i, was calculated as:

$$L_{\mathrm{suit}}(i,j) = H_{\mathrm{norm}}(i,j) \times S_{\mathrm{norm}}(i,j) \times C_{\mathrm{norm}}(i,j) \times ST_{\mathrm{norm}}(i,j), \quad (3)$$

where $H_{\mathrm{norm}}(i,j)$, $S_{\mathrm{norm}}(i,j)$, $C_{\mathrm{norm}}(i,j)$, and $ST_{\mathrm{norm}}(i,j)$ refer to altitude, slope, climatic maximum potential productivity, and soil texture after the normalization of grid j in province i, respectively. LSC decreases with increasing altitude and slope and rises with increasing climate production potential and soil texture. $C_{\mathrm{norm}}(i,j)$ is calculated from eq. (1), while $H_{\mathrm{norm}}(i,j)$ and $S_{\mathrm{norm}}(i,j)$ are calculated from eq. (2). $ST_{\mathrm{norm}}(i,j)$ is calculated from eqs. (1) or (2) according to the positive/negative correlation between the content of sand, silt, and clay in the soil and the modern land reclamation rate (Zhang, 2020).

3.2.3 Gridding allocation method for cropland

The value of LSC is calculated on the basis of eq. (3). Different limiting factors restrict the distribution of cropland in different regions. Thus, China is divided into three regions (eastern China, Xinjiang, and Qinghai-Xizang) to devise the gridding allocation method for cropland areas.

The historical distribution of cropland cover for eastern China is restricted by its coastline, the northern boundary of the FPE, and the LSC. Since the Song Dynasty, the coastlines in eastern China have undergone many changes. In particular, the historical coastlines of the western coast of Bohai Bay, the northern coast of Jiangsu, and the Yangtze estuary were higher than the present-day coastlines (Figure 1a). However, the maximum extent of cropland cover determined in this study was based on the current coastline. This condition indicates that cropland might be allocated to the sea in

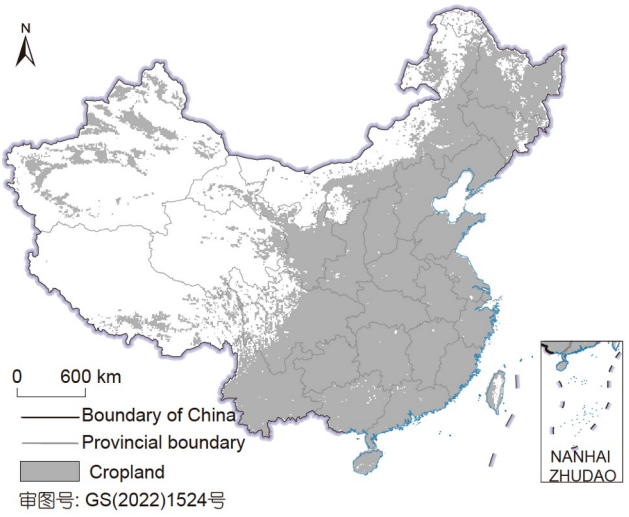

Figure 4 Maximum extent of cropland cover in China.

the gridding allocation of cropland. Thus, the gridding allocation method introduced historical coastlines as a limiting factor. The FPE was mainly distributed in northern China and frequently changed throughout history (Figure 1b). The distribution of historical cropland should not exceed the northern boundary of the FPE. However, the maximum extent of cropland synthesized based on remote sensing-derived cropland data was far beyond the northern boundary of the historical FPE. Thus, the northern boundaries of the FPE in different periods were regarded as the boundary of cropland cover in this study. $\text{Cropland}_{\text{east}}(j, t)$, the cropland area in grid j in year t, was calculated as:

$$\text{Cropland}_{\text{east}}(j, t) = \alpha \times \beta \times \gamma \times \frac{L_{\text{suit}}(i,j)}{\sum_i L_{\text{suit}}(i,j)} \times \text{Area}_{\text{crop}}(i, t), \quad (4)$$

where $L_{\text{suit}}(i, j)$ is the LSC value of grid j of province i; $\text{Area}_{\text{crop}}(i, t)$ is the cropland area of province i in year t; α, β, and γ are the indexes of the maximum extent of cropland, coastlines, and the northern boundary of the PFE, respectively. If the area of grid j exceeds 50% of the maximum extent of cropland, coastline, or the northern boundary of the FPE, then α, β, and γ are assigned to zero, respectively; otherwise, the values are one.

Xinjiang is an inland arid area located on the northwest border of China and includes a mixture of agriculture and animal husbandry. The historical agricultural development in Xinjiang primarily involved the land reclamation of the oasis in the Central Plains dynasties. Historical documents suggest that agriculture and animal husbandry in Xinjiang are mainly in the south and north of the Tianshan Mountains, respectively, before the Qing Dynasty. Moreover, agriculture coexisted in the south and north of the Tianshan Mountains, with emphasis on the north since the Qing Dynasty (Zhang, 2017). The southern, northern, and eastern areas of Xinjiang were taken as the basic unit and the land reclamation index was introduced as the limiting factor in the gridding allocation of cropland in Xinjiang to reflect changes in cropland cover objectively. $\text{Cropland}_{\text{XJ}}(j, t)$, which refers to the cropland area of Xinjiang in grid j in year t, was calculated as:

$$\text{Cropland}_{\text{XJ}}(j, t) = \alpha \times \delta \times \frac{L_{\text{suit}}(i,j)}{\sum_i L_{\text{suit}}(i,j)} \times \text{Area}_{\text{crop}}(i, t), \quad (5)$$

where δ denotes the index of land reclamation. If grid j is within the scope of land reclamation in Xinjiang, then δ is assigned to one; otherwise, the value is zero. The other parameters have the same meaning as in eq. (4).

The Qinghai-Xizang region is located in southwest China. Compared with the other regions, Qinghai-Xizang has less arable land, and the cropland is mainly distributed in river valleys. The gridding allocation method for cropland in Qinghai-Xizang was devised on the basis of the maximum extent of cropland and the LSC:

$$\text{Cropland}_{\text{QT}}(j, t) = \alpha \times \frac{L_{\text{suit}}(i,j)}{\sum_i L_{\text{suit}}(i,j)} \times \text{Area}_{\text{crop}}(i, t), \quad (6)$$

where $\text{Cropland}_{\text{QT}}(j, t)$ denotes the cropland area of Qinghai-Xizang in grid j in year t, and the other parameters have the same meaning as in eq. (4).

Notably, few grids at the resolution of 10 km are filled by cropland according to the above method. This finding is inconsistent with land use facts. An analysis of the remote sensing-based crop cover data in the AD 1980 at 10 km suggests that the proportion of grids with the fractional cropland area (FCA) exceeding 90% is only 1.07%. Therefore, the historical FCA at the gird scale should not exceed 90%. Thus, 90% was set in the allocation process as the maximum FCA value for 10 km grids. When applying the gridding allocation method, all the excess area were removed and a loop allocate was implemented until all the grids met the prescribed limit of 90% (Li et al., 2016).

4. Results

Using the gridding allocation method in this study, a total and 25 provincial cropland areas were obtained across China, and the spatial distribution of cropland cover for 24 time slices over the last millennium was mapped at a resolution of 10 km. The spatiotemporal changes in cropland were then analyzed, and the reliability of the cropland area reconstruction method was evaluated.

4.1 Total cropland area for China

The changes in cropland area across China between AD 1000

and 1999 are illustrated in Figure 5. The reconstruction shows fluctuating increase trends across China during the entire period. The total cropland area across China increased from 3.71×10^7 ha in AD 1000 to 12.92×10^7 ha in AD 1999. The cropland area peaked at 13.50×10^7 ha in the AD 1980. FCA increased by 2.5 times from 3.85% to 13.14% over this period. Changes in cropland over the past millennium can be divided into three phases: fluctuation without considerable net change between AD 1000 and 1290 (P1), a slow increase between AD 1290 and 1661 (P2), and a rapid increase between AD 1661 and 1999 (P3). The three stages are then comprehensively described.

During P1, the total cropland area in China fluctuated while maintaining stability overall. The total cropland area exhibited a fluctuating change process from increasing to decreasing and then increasing and decreasing again between the 10th and 13th centuries. These changes were closely related to confrontation and regime change. During this period, China was ruled by the Liao, Northern Song, Southern Song, and Jin dynasties and some local regimes and tribal entities (Dali, Western Xia, Western Liao, and Black Khan). Cropland expanded and shrank along with the rise and fall of these regimes. For example, the war between the Song and Liao Dynasties, which started in the late 10th century, severely damaged the agriculture of the central plain in China. At the end of the war, the Chanyuan Alliance armistice was formed in AD 1004, society gradually stabilized, and agriculture was developed. Accordingly, the total cropland area increased from 3.71×10^7 ha at the end of the 10th century to 5.13×10^7 ha in AD 1078. Subsequently, after the control of eastern China transitioned from the Liao to the Jin Dynasty, wars between the Southern Song and Jin Dynasties, which lasted for decades, resulted in the abandonment of large cropland areas in northern China and even the Jianghuai region. Consequently, the cropland area decreased sharply to 3.91×10^7 ha in AD 1162. After establishing the Longxing Peace Treaty in AD 1163, the government enacted a series of policies to promote immigration and land cultivation, and the total cropland area increased to 5.23×10^7 ha in AD 1215. However, the Mongolians gradually unified eastern China from AD 1234 to 1271 by conquering the Jin and Southern Song Dynasties. The war lasted for over half a century, leading to a population decline of approximately 60 million (Wu, 2000). In this case, the cropland area rapidly decreased to 4.25×10^7 ha in AD 1290.

The cropland area slowly increased during P2. After Mongolians unified China, the government rejected the motion that drove out all the Chinese Han people and converted croplands into pastures. Instead, they prioritized the development of agriculture and prohibited converting farming into pastures. These policies promoted the transformation of society from nomadic to agricultural. After the regime changed from the Yuan to the Ming Dynasty, the Ming

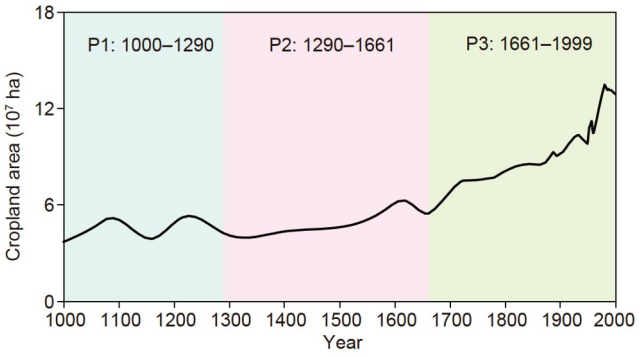

Figure 5 Total cropland area across China from AD 1000 to 1999.

government implemented policies related to immigration and reclamation to recover agricultural land after the war. Consequently, social stability and population growth allowed the cropland area to increase from 4.25×10^7 ha in the early Yuan Dynasty to 5.71×10^7 ha (AD 1583) and 6.27×10^7 ha (AD 1620), representing an increase of approximately 2.02×10^7 ha at an annual average growth rate of 0.14%.

The cropland area rapidly increased during P3. Rapid population growth was accompanied by large-scale cropland expansion during this period. After the Qing Dynasty was established, the population increased from less than 1.50×10^8 in the early Qing Dynasty to over 3.00×10^8 and 4.00×10^8 in the late Qianlong period and the Daoguang period, respectively (Cao, 2001). Simultaneously, the total cropland area also increased from 5.47×10^7 ha (AD 1661) to 8.42×10^7 ha (AD 1820) and 9.72×10^7 ha (AD 1913). This phenomenon translates to an increase of 4.25×10^7 ha and an average annual growth rate of 0.31% over more than 250 years. After the People's Republic of China was founded, the population continuously increased and reached 12.95×10^8 by AD 2000. Accordingly, the cropland area increased from 9.81×10^7 ha (AD 1949) to 12.92×10^7 ha (AD 1999), corresponding to an increase of approximately 3.11×10^7 ha and an average annual growth rate of 0.64% over 50 years.

4.2 Provincial cropland area for China

Figure 6 illustrates the changes in cropland areas in the 25 Chinese provincial areas over the past millennium. The cropland area of each province shows a fluctuating increase trend, but considerable differences still exist among provinces.

The trends in cropland area in the middle and lower reaches of the Yellow River (i.e., Shaanxi, Shanxi, Jing-Jin-Ji, and Shandong), along with the middle and lower reaches of the Yangtze River (i.e., Anhui, Hu-Ning, Hubei, and Chuan-Yu), were similar to the overall trend in China (i.e., fluctuations with an overall increase in cropland area). The cropland area in some provinces in northeastern China

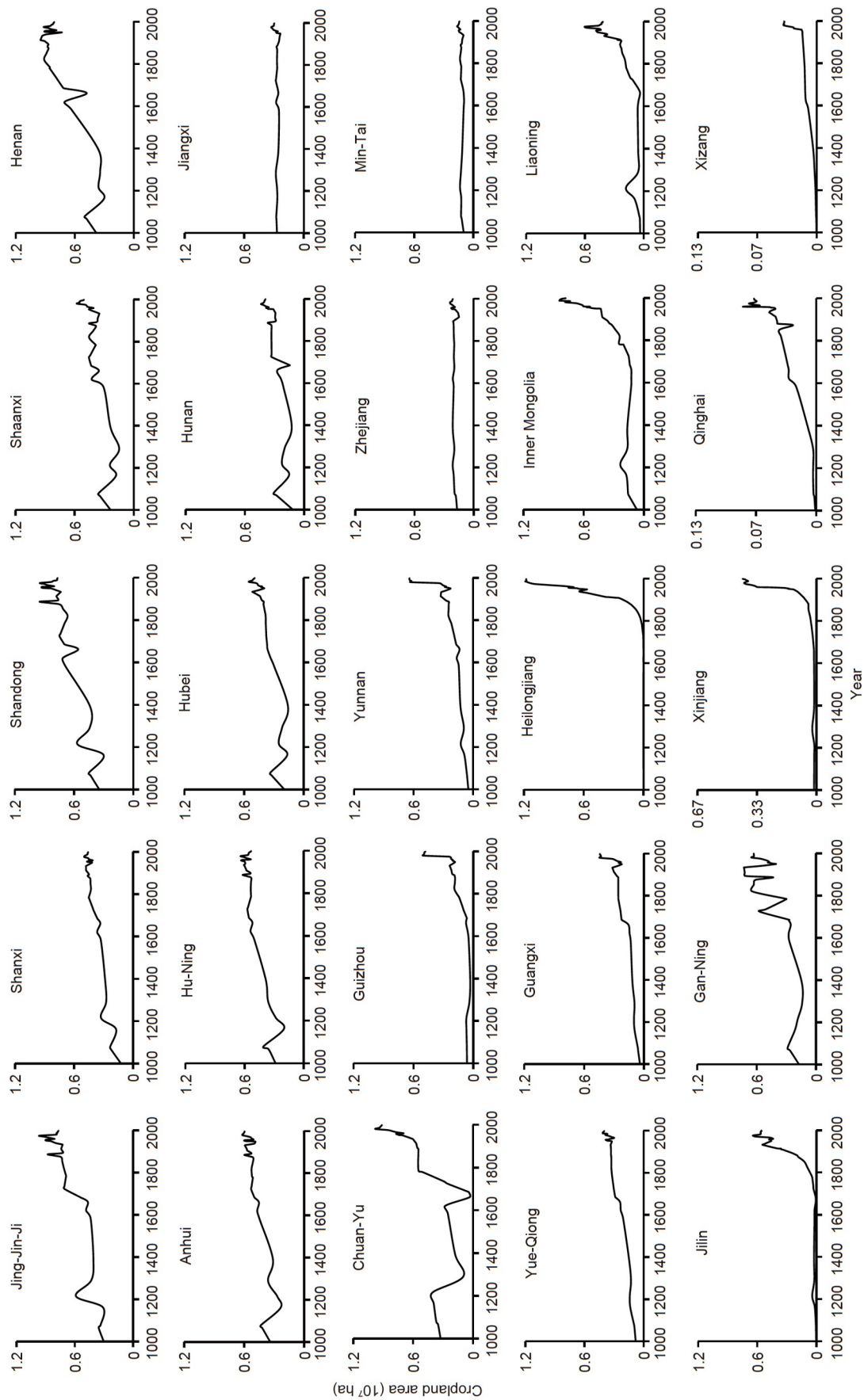

Figure 6 Provincial cropland area across China from AD 1000 to 1999.

(Liaoning, Jilin, Heilongjiang, and Inner Mongolia), northwestern China (Gan-Ning, Qinghai, and Xinjiang), and parts of southwestern China (Guizhou and Yunnan) slightly varied before the Qing Dynasty and rapidly increased after this dynasty. Meanwhile, the cropland area steadily increased in the southern coastal region of China (Min-Tai, Yue-Qiong, and Guangxi).

Figure 7 shows the proportions of provincial cropland area out of the total cropland area for different periods from AD 1000 to 1999. In the early Northern Song Dynasty (AD 1000), among provincial areas, Henan Province had the largest cultivated land area (0.38×10^7 ha, accounting for 10.30% of the total cropland area), followed by the Shandong and Anhui Provinces (accounting for 9.27% and 9.16% of the total cropland area, respectively). In AD 1000, the proportions of provincial cropland area in northeastern (i.e., Heilongjiang, Jilin, and Liaoning) and western (i.e., Qinghai, Xinjiang, and Xizang) China were less than 1.00%. Among all provinces, Xizang had the smallest proportion of provincial cropland (0.01%). In the early Qing Dynasty (AD 1661), Shandong had the highest provincial cropland area among all provincial areas (0.56×10^7 ha, accounting for 10.19% of the total cropland area), followed by Hu-Ning and Henan (9.51% and 8.75% of the total cropland area, respectively). Simultaneously, the proportions of cropland area in the northeastern and western provinces remained less than 1.00%, reflecting limited agricultural development in these areas. By the end of the 20th century (AD 1999), Heilongjiang Province had the largest provincial cropland area in China (1.18×10^7 ha, accounting for 9.11% of the total cropland area), followed by Chuan-Yu (0.91×10^7 ha, 7.06%). Only Qinghai and Xizang had proportions of cropland area less than 1.00% (0.53% and 0.28%, respectively).

4.3 Spatial distribution of cropland cover in China

4.3.1 Overview of the spatial distributions of cropland cover

Figure 8 illustrates the spatial distribution of cropland across China from AD 1000 to 1999. The cropland in China is mainly distributed in the eastern monsoonal zone. The scope of land reclamation over the last millennium expanded continuously with population growth and technological advancement. The cultivated land was first concentrated in the middle-lower reaches of the Yellow and Yangtze Rivers and then expanded to the surrounding areas and even to the frontier areas. The grid cells covered by cropland accounted for 32.01% (AD 1000) and 48.52% (AD 1999) of all grid cells. Simultaneously, the total FCA gradually increased by 2.5 times from 3.85% at the end of the 10th century to 13.49% at the end of the 20th century. Specifically, the FCAs of the middle-lower reaches of the Yellow and Yangtze Rivers, which are the main traditional agricultural areas in China, increased by 1.38 times and 0.83 times from 15.35% and 18.89% to 36.54% and 27.32%, respectively.

Figure 9 shows the proportions of cropland area in different topographic units out of the total cropland area (data of plains, hills and low mountains, and middle and high mountains were obtained from 1:1 million Chinese geomorphologic atlas, available at http://www.resdc.cn). Cropland was mainly distributed in the plains, accounting for 52.99–68.12% of the total cropland area, followed by the hills and low mountains (18.88–29.92%). Cropland distributed in the middle and high mountains only accounted for 11.34–17.58% of the total cropland area. The proportion of cropland in the plains decreased by approximately 16.95% as the cropland area increased over the past millennium. By contrast, the proportions of cropland increased by 23.05% in the hills and low mountains and by 43.79% in the middle and high mountains. These trends reflect land reclamation expansion from plains to mountains and hills over the last millennium.

4.3.2 Changes in the spatial distributions of cropland cover

The spatial changes in cropland cover in different periods over the past millennium in China were analyzed in accordance with the stages of the increasing trend in the total

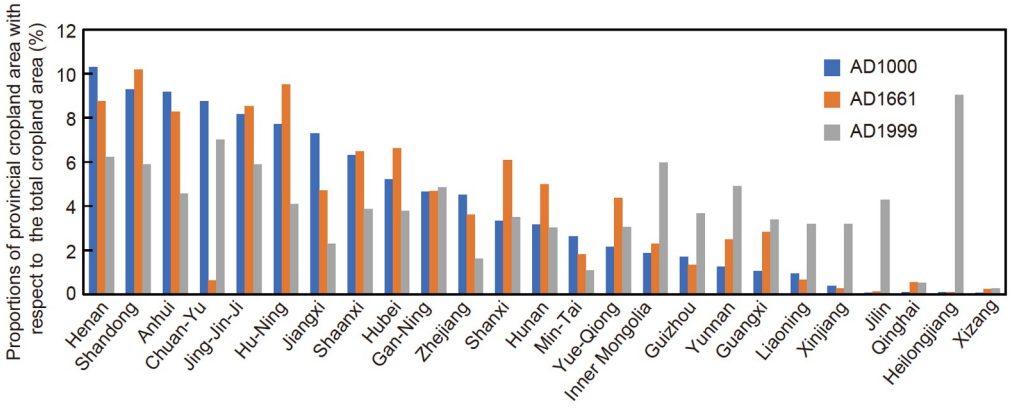

Figure 7 Proportions of provincial cropland area out of the total cropland area.

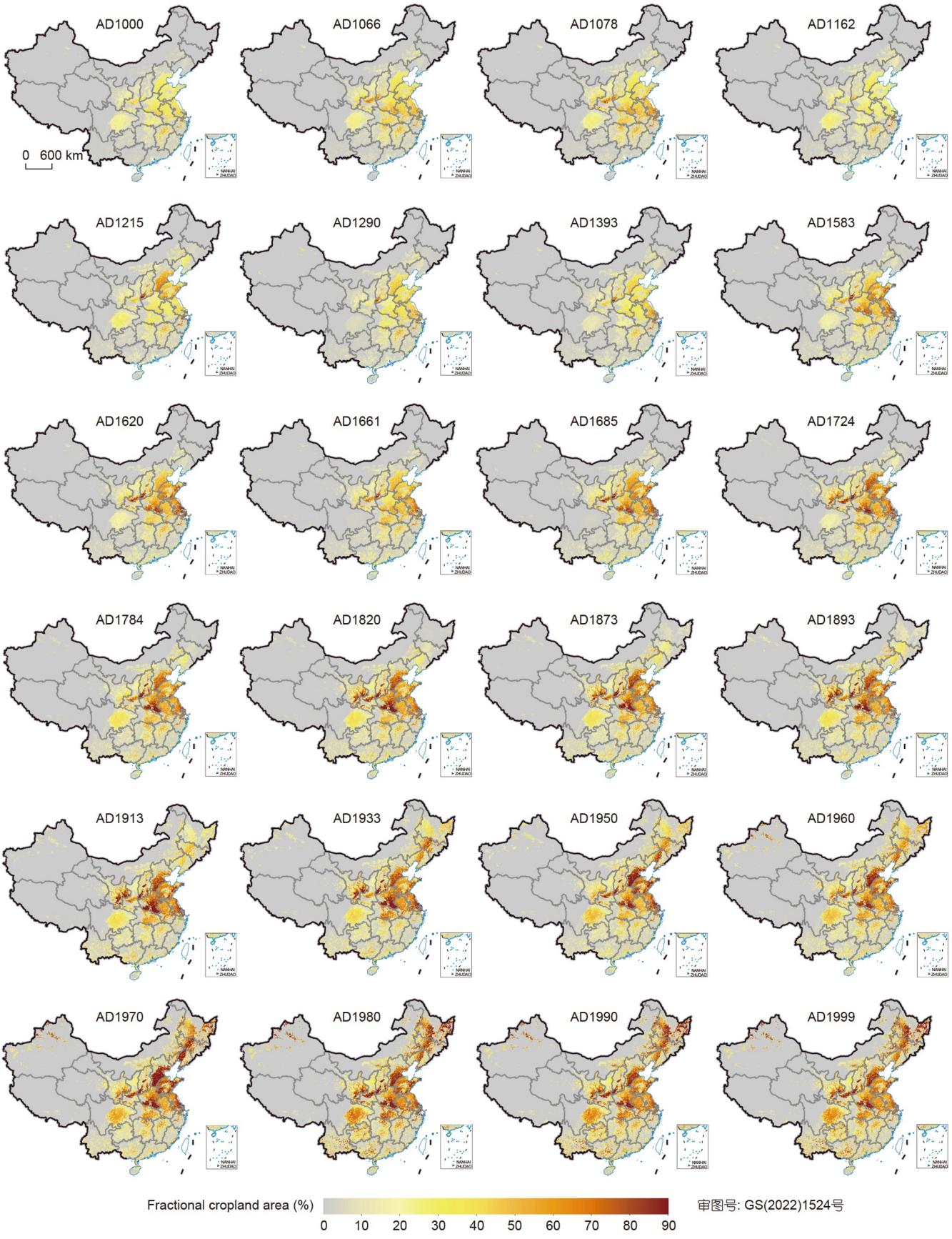

Figure 8 Spatial distribution of cropland cover in China over the past millennium at a 10 km resolution.

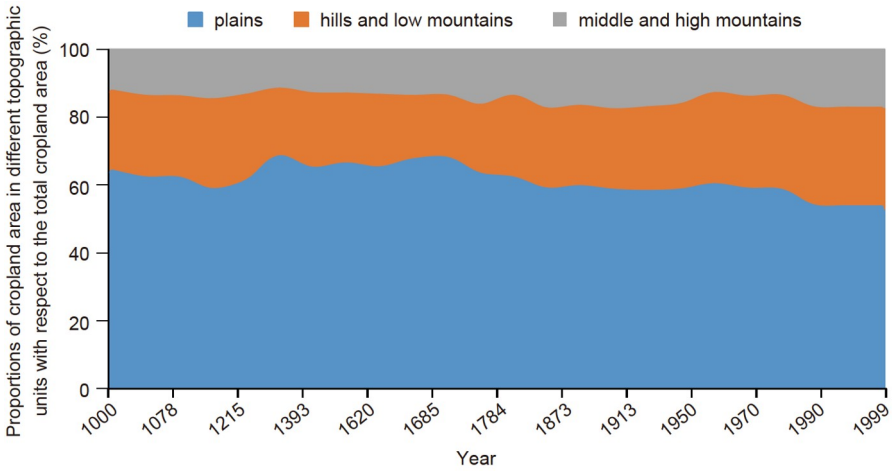

Figure 9 Proportions of cropland area in different topographic units out of the total cropland area.

cropland area in Section 4.1. These changes can be summarized in the following three phases.

(1) During P1 (AD 1000–1290), the changes in FCA mainly occurred in central and eastern China. FCA increased significantly in southern China, especially in the middle and lower reaches of the Yangtze River. This increase is primarily due to wars between the Song, Liao, and Jin Dynasties after the An-Shi Rebellion, forcing the population in northern China to migrate southward and reversing the long-term pattern of the population (i.e., high and low populations in the north and south, respectively). Specifically, taking the Qinling Mountain-Huaihe River as the boundary, the proportion of China's population in the south increased from 56.90% in AD 980 to 62.60% in AD 1078, while that in the north decreased from 43.10% to 37.40% (Wu, 2000).

The total FCA increased from 3.85% (AD 1000) to 5.33% (AD 1078) during the Song and Liao Dynasties. This period involved the formation of the Chanyuan Alliance armistice in AD 1004 and rapid population growth. Specifically, dynamic agricultural (e.g., polder and terrace agriculture) developments were driven by large-scale immigration southward; thus, competing with open water and mountain areas for cultivated land was normalized. At this time, the FCAs in the middle-lower reaches of the Yangtze and Yellow Rivers increased from 14.89% and 15.35% (AD 1000) to 21.27% and 20.77% (AD 1078), corresponding to increases of 42.85% and 35.31%, respectively (Figure 10a). Consequently, the middle-lower reaches of the Yangtze River replaced the middle-lower reaches of the Yellow River to become the economic center of China during this time. This finding indicates that the government revenue mainly came from the south, especially from the southeast. The FCA in eastern China declined significantly because of wars when the Southern Song Dynasty replaced the Northern Song Dynasty (Figure 10b). The FCAs in the middle-lower reaches of the Yangtze and Yellow Rivers decreased by 32.43% and 37.59%, respectively. Specifically, the FCAs in the Hu-Ning, Anhui, Henan, Shandong, and Hubei provinces decreased by 51.09%, 45.67%, 39.40%, 33.41%, and 50.96%, respectively.

After signing the Longxing Peace Treaty, Chinese society gradually stabilized and agricultural production rapidly recovered. In northern China, the Jin government enacted a series of policies to promote land reclamation. The FCAs in the middle and lower reaches of the Yellow River increased from 14.03% (AD 1162) to 23.03% (AD 1215). Figure 10c shows that the FCAs of the Shandong, Jing-Jin-Ji, and Shanxi Provinces were 0.89, 0.89, and 0.88 times larger in AD 1215 than in AD 1162, respectively. However, the war between the Southern Song and Yuan Dynasties lasted for more than half a century, leading to an 18.67% reduction in total FCA. Notably, compared with those in the Southern Song Dynasty (AD 1215), the FCAs in the middle and lower reaches of the Yellow River and the Sichuan Basin were 21.31% and 75.87% lower in AD 1290, respectively (Figure 10d). Other regions outside of central and eastern China that were only slightly affected by the war were characterized by harsh geographical environments and limited arable land. Thus, the FCAs in most areas remained relatively low despite the increase in cropland areas in these regions. For example, the FCA was between 4% and 6% in southern coastal China and less than 5% in southwestern China, while the FCAs in northeastern China, northwestern China, and the Qinghai–Tibet Plateau were less than 3%, 1.5%, and 0.05%, respectively.

(2) During P2 (AD 1290–1661), agriculture was developed on previously abandoned land, primarily in traditional agricultural areas, especially in central and eastern China. The Yuan Dynasty was established for nomadic peoples; however, the government attached considerable importance to agricultural production, and FCA increased rapidly. The economies of the Yuan and Ming Dynasties were dominated

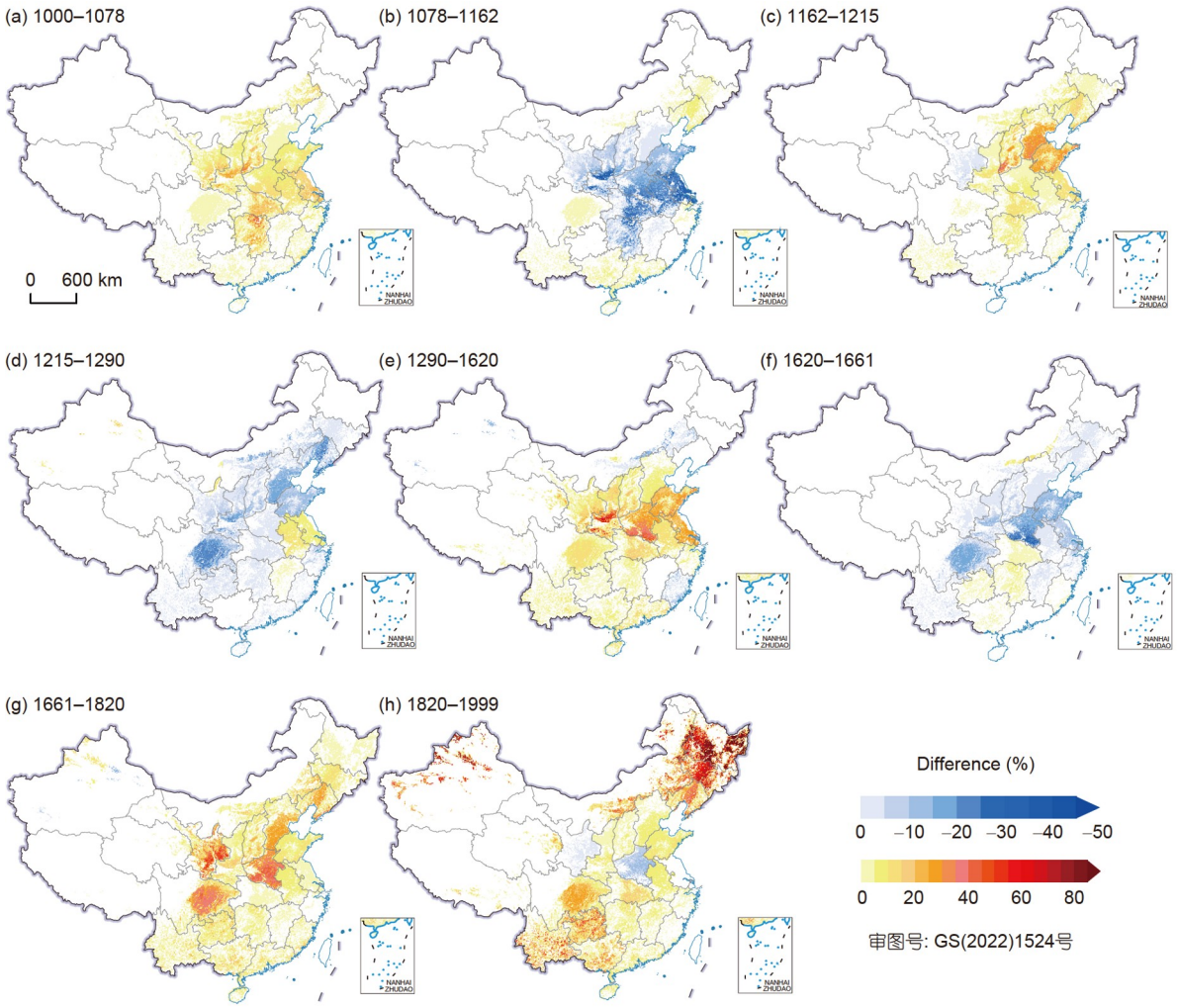

Figure 10 Changes in fractional cropland area of China during different periods.

by agriculture. The total FCA increased by 47.46% from AD 1290 to 1620. During this period, the FCAs in the middle-lower reaches of the Yellow and Yangtze Rivers increased to 29.80% and 22.39%, corresponding to increases of 64.46% and 27.86%, respectively. The FCA in the Sichuan Basin increased nearly two times, from 5.16% in AD 1290 to 14.78% in AD 1620 (Figure 10e). However, the subsequent regime shift from the Ming to the Qing Dynasty led to a decline in FCA in the above-mentioned agricultural areas. For example, the FCAs of Henan, Shandong, and Chuan-Yu decreased by 32.02%, 21.91%, and 87.85%, respectively, from the end of the Ming dynasty (AD 1620) to the early Qing Dynasty (AD 1661; Figure 10f). Conversely, the FCAs of Hunan, Hubei, and Guizhou increased by 15.75%, 9.37%, and 30.20%, respectively, during this period. Throughout this period, the land reclamation in other areas was consistent with the previous period. Thus, the cropland area fluctuated while generally remaining stable. For example, the FCAs in the southern coastal area of China and the Qinghai-Xizang region increased by 5.01% and 2.54%, respectively, while the FCA in northwestern China decreased by 4.76%.

(3) P3 (AD 1661–1999) was characterized by continuous land reclamation in the inland plains and the vigorous expansion of land reclamation in areas with low reclamation rates (i.e., the mountainous areas and their surroundings). This phenomenon is due to the rapid increased population from 1.60×10^8 at the end of the 17th century to 4.00×10^8 at the middle of the 19th century and 12.6×10^8 at the end of the 20th century (Cao, 2001). Therefore, a massive amount of cropland had to be created to support the large population. Meanwhile, with the popularization of drought-tolerant and high-yield crops (e.g., corn and potatoes) from abroad starting in the late Ming Dynasty, farming was no longer limited by the natural conditions of some areas, resulting in the expansion of arable land. Thus, the pattern of land reclamation in China has begun to diverge from the original pattern of cropland cover, with cropland area expanding to areas of low reclamation in southwest, northeast, and

northwest China and advancing from the plains and valleys to the hills and mountains.

After the Revolt of the Three Feudatories in southwestern China, the government implemented reform measures that included the bureaucratization of native officers and immigration from Hunan, Hubei, and surrounding areas to the Sichuan Basin. These policies resulted in an influx of agricultural people into southwest China for land reclamation. The FCA in this region increased from 2.13% in the early Qing Dynasty (AD 1661) to 8.66% in the middle Qing Dynasty (AD 1820), 10.20% during the Republic of China period (AD 1933), and 18.00% in AD 1999 (Figure 10g and 10h), demonstrating an increase of 7.5 times over 300 years. The government implemented a policy prohibiting reclamation in northeast China (the birthplace of the Qing Dynasty) before the mid-19th century. Subsequently, faced with demographic and socioeconomic pressures, the Qing government removed the restriction on reclamation in northeast China and encouraged immigration into the borderlands. Consequently, northeast China became one of the most important agricultural areas in the country (Figure 10h). The FCA in this area increased from 0.55% in AD 1661 to 3.90% in AD 1820, 18.59% in AD 1933, and 26.61% in AD 1999, corresponding to an increase of 47.4 times over 300 years. Northwest China is a typical arid area, and the natural conditions of this region are not conducive to agricultural development. However, this area has become a major migration destination since the Qing Dynasty. In particular, the population of Xinjiang increased from 1.392×10^6 in AD 1880 to 2.169×10^6 in AD 1910, 4.762×10^6 in AD 1953, and 17.633×10^6 in AD 1999 (Cao, 2001; Hou, 2001). Xinjiang became the center of agricultural production in northwest China. A large amount of grassland in Xinjiang was transformed into farmland (Figure 10h), and the FCA increased 26.8 times from 0.09% in AD 1661 to 2.50% in AD 1999.

4.4 Reliability analysis of our reconstruction

The reconstruction results were verified through qualitative analysis and quantitative evaluation. The consistency between the spatiotemporal change in cropland reflected by reconstruction and data obtained from historical documents was qualitatively analyzed. As shown in Sections 4.1–4.3, the reconstruction results revealed the spatiotemporal changes in historical cropland.

No historical 'true values' exist for the spatial patterns of cropland cover; thus, an indirect quantitative method was used to analyze the reliability of the grid reconstruction results. Provincial cropland areas (AD 1980) were allocated into grids using the devised method. The allocation results were then compared with the current cropland grid data based on remote sensing images to verify the feasibility of the proposed approach and the reliability of the reconstruction results. As shown in Figure 11a and 11b, the spatial pattern of reconstructed cropland cover generally agrees with the distribution derived from remote sensing data. Negative differences (i.e., where the reconstructed cropland area is less than that obtained from remote sensing images) were primarily distributed in the Sichuan Basin and northwestern Jing-Jin-Ji. Positive or negative values were not concentrated in other regions (Figure 11c).

A larger absolute value of difference corresponded to a small percentage of grid cells (Table 2). Grid cells with absolute differences of 0–10% and 10–20% accounted for 70.35% and 13.65% of all grid cells, respectively. Moreover, grids with differences exceeding 60% accounted for only 0.83% of all grid cells, indicating the reliability of the reconstruction method. The reconstruction results also objectively revealed the spatiotemporal changes of cropland in the historical period.

5. Discussion

5.1 Gridding reconstruction method for cropland

Gridding reconstruction is one of the most critical tools for historical cropland reconstruction. Therefore, the rationality of gridding reconstruction has received considerable academic attention. Reconstruction models can be classified into spatial allocation and spatial evolution models. Compared with spatial evolution models, spatial allocation models are characterized by fewer parameters and easy data acquisition. Therefore, spatial allocation models are practical for reconstructing cropland cover at large spatiotemporal scales (He et al., 2019). Thus, a spatial allocation model was used in this study. Specifically, the maximum extent of cropland was first determined on the basis of multiple remote sensing-derived cropland data. The model of LSC was then built, and the gridding allocation method for provincial cropland was devised in consideration of the major factors driving and limiting the spatial distribution of cropland cover. The allocation model was applied to provincial cropland area data to reconstruct 10 km cropland cover maps of China for AD 1000–1999.

However, as mentioned in Section 3.2, gridding reconstruction depends on selecting and quantifying driving and limiting factors. Many factors can influence the distribution of cropland cover, including natural (e.g., light, precipitation, altitude, slope, soil organic matter, and natural water systems) and human (e.g., population settlement, transportation, and cropland irrigation) factors. Although the above factors have different effects on cropland distribution, fully considering all these factors will undoubtedly improve the reliability of the reconstruction results. However, obtaining historical data involving large areas, long periods,

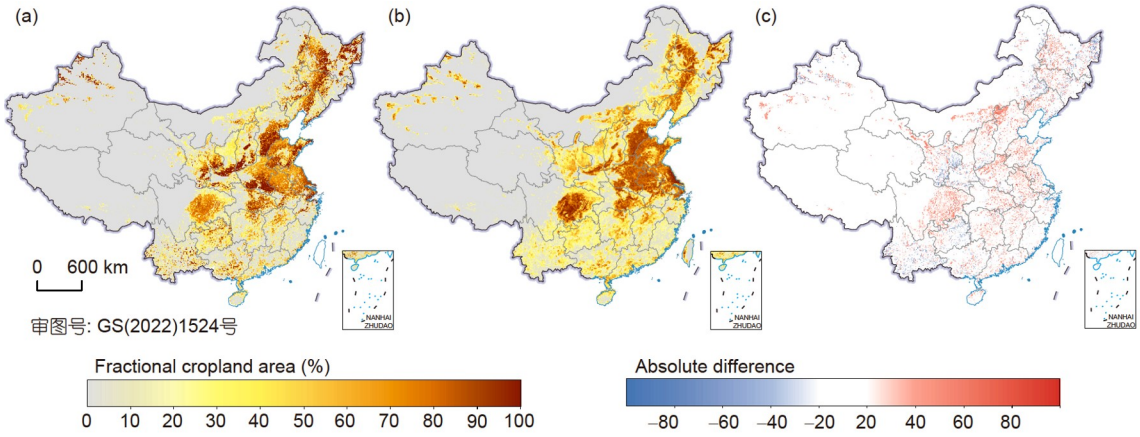

Figure 11 Spatial patterns of cropland cover in AD 1980: proposed reconstruction (a), CLUDs (b), and the difference between them (c).

Table 2 Differences in cropland cover in AD 1980 between the proposed reconstruction and CLUDs

Difference (%)	Percentage (%)	Difference (%)	Percentage (%)
<−80	0.04	0–10	17.57
−80–−70	0.11	10–20	10.36
−70–−60	0.21	20–30	5.99
−60–−50	0.37	30–40	2.95
−50–−40	0.66	40–50	1.38
−40–−30	1.17	50–60	0.7
−30–−20	1.95	60–70	0.32
−20–−10	3.29	70–80	0.12
−10–0	52.78	> 80	0.03

and high resolution is often challenging. Thus, these data are often replaced by modern data in the quantification process. This condition raises a serious problem: some historical data can be replaced with modern data while other data cannot. Therefore, the concept of the "relative stability factors" was introduced in this study. This concept means that some factors (e.g., light, precipitation, elevation, slope, and soil texture) remain unchanged over time in the study area, and these factors can be replaced by modern data. Other factors (e.g., rivers, soil organic matter, roads, and settlements) that are easily changed or have changed considerably over time should not be replaced by modern data because such a replacement would induce the deviation of reconstruction results from reality. Thus, the selected potential maximum productivity of climate, soil texture, altitude, and slope was include in the LSC calculation. These factors were assumed to be relatively stable and were directly substituted by modern data.

Notably, models of the cropland spatial distribution based on natural factors have an inherent defect. That is, a grid is allocated cropland as long as the LSC value of the grid is larger than zero and the grid is within the maximum distribution extent of cropland. However, the grid may not have the distribution of cultivated land. Avoiding this disadvantage in areas with low LSC values is difficult. One way to solve this problem is to consider human factors supported by historical data in the model. For instance, Wu et al. (2020) reconstructed the distribution of cropland cover in northeast China based on historical settlement data. This method effectively reduced the deviation and provided a valuable example for the gridding reconstruction of cropland at large spatiotemporal scales.

5.2 Comparison with global historical land use datasets

At present, the primary global historical land use datasets containing cropland data for the past millennium are HYDE and PJ. Some regional research results covering the last 300 years are included in HYDE 3.2. However, most regional cropland data in this global dataset were estimated using population and per capita cropland. LSC in this dataset was determined by combining various human and natural factors, such as population and climate. Finally, the cropland area of each region was allocated to the grid cell. The PJ dataset for 1700–1992 was constructed on the basis of HYDE and SAGE datasets. The PJ dataset for AD 800–1700 was reconstructed using the cropland distribution pattern in AD 1700 as a benchmark and population as a proxy. By

contrast, the cropland area at the provincial (e.g., Lu and Dao) level at multiple time slices served as the data source of gridding allocation in this study. These cropland data were reconstructed using Chinese historical tax records for cropland areas and relevant historical documents. The LSC and gridding allocation models for cropland were developed in consideration of the dominance, stability, and availability of factors related to the distribution of cropland. Overall, the data source and methodology in this study were reliable. Thus, the results should also be more reliable than the global datasets. A detailed comparison between the global datasets and the proposed reconstruction will be presented in another article.

6. Conclusions

LSC and cropland allocation models were developed considering the altitude, slope, potential maximum productivity of climate, and soil texture by utilizing historical document-based provincial cropland data. Using this approach, the cropland cover in China for 24 years over the last millennium was reconstructed at a spatial resolution of 10 km. The main conclusions are as follows:

Cropland area in China has shown fluctuating increase trends over the last millennium. The total cropland area in China increased from 3.71×10^7 ha in AD 1000 to 12.92×10^7 ha in AD 1999, a net increase of 9.21×10^7 ha. The changes in cropland cover can be described in three phases: a period of fluctuation but overall stability (AD 1000–1290), a period of slow increase (AD 1290–1661), and a period of rapid increase (AD 1661–1999). The cropland area peaked at 13.50×10^7 ha in the AD 1980.

Over the last millennium, agricultural development was first concentrated in the middle-lower reaches of the Yellow and Yangtze Rivers and then expanded to the surrounding hills and mountains and even to the frontier areas. The FCA of the middle and lower reaches of the Yellow River increased 1.38 times from 15.35% (AD 1000) to 36.54% (AD 1999), while that of the middle and lower reaches of the Yangtze River increased 0.83 times from 14.89% to 27.32%.

Since the mid-Qing Dynasty, the arable lands in southwest, northeast, and northwest China have been continuously cultivated along with the rapid population growth and the introduction of drought-tolerant and high-yield crops from abroad. The FCAs in these areas increased from 2.13%, 0.55%, and 0.09% in AD 1661 to 18.00%, 26.61%, and 2.50% in AD 1999, respectively. From AD 1661 to 1999, the increase in proportions of cropland was 55.04% in the hills and low mountains and 26.61% in the middle and high mountains, while that of cropland in the plains decreased by 21.15%.

The reconstructed spatial distribution of cropland cover generally agrees with the data from historical documents. When comparing the reconstructed gridding cropland to the 1980 data derived from remote sensing images, 70.35% of all grid cells had absolute differences with the remote sensing data of less than 10%, while grids with differences exceeding 60% accounted for only 0.83% of all grids. Thus, the cropland cover reconstructed in this study can objectively reproduce the historical spatial patterns of cropland cover.

Acknowledgements *This work was supported by the National Key Research and Development Program of China (Grant No. 2017YFA0603304) and the Chinese Academy of Sciences Strategic Priority Research Program (Grant No. XDA19040101).*

References

An C B, Zhang M, Wang W, Liu Y, Duan F T, Dong W M. 2020. The pattern of Xinjiang physical geography and its relationship with the temporal-spatial distribution of agriculture and husbandry (in Chinese). Sci Sin Terrae, 50: 295–304

Cao S J. 2000. Population History of China. Vol. 4 (in Chinese). Shanghai: Fudan University Press. 240–247

Cao S J. 2001. Population History of China. Vol. 5 (in Chinese). Shanghai: Fudan University Press. 691–719

Ellis E C, Kaplan J O, Fuller D Q, Vavrus S, Klein Goldewijk K, Verburg P H. 2013. Used planet: A global history. Proc Natl Acad Sci USA, 110: 7978–7985

Fang X, Zhao W, Zhang C, Zhang D, Wei X, Qiu W, Ye Y. 2020. Methodology for credibility assessment of historical global LUCC datasets. Sci China Earth Sci, 63: 1013–1025

Fuchs R, Herold M, Verburg P H, Clevers J G P W, Eberle J. 2015. Gross changes in reconstructions of historic land cover/use for Europe between 1900 and 2010. Glob Change Biol, 21: 299–313

Fuchs R, Herold M, Verburg P H, Clevers J G P W. 2013. A high-resolution and harmonized model approach for reconstructing and analysing historic land changes in Europe. Biogeosciences, 10: 1543–1559

Ge Q S, Dai J H, He F N, Pan Y, Wang M M. 2008. Land use changes and their relations with carbon cycles over the past 300 a in China. Sci China Ser D-Earth Sci, 51: 871–884

Ge Q, Dai J, He F, Zheng J, Man Z, Zhao Y. 2004. Spatiotemporal dynamics of reclamation and cultivation and its driving factors in parts of China during the last three centuries. Prog Nat Sci, 14: 605–613

Guo R, Liu F G, Chen Q, Zhou Q, Gu X J, Cai X C M. 2021. Reconstruction of cultivated land pattern in the upper reaches of the Yellow River in the late Northern Song Dynasty: Take Hehuang Valley as an example (in Chinese). J Nat Reso, 36: 27–36

Han M L. 2012. Historical Agricultural Geography of China (in Chinese). Beijing: Peking University Press. 13–47

He F, Li M, Li S. 2017. Reconstruction of Lu-level cropland areas in the Northern Song Dynasty (AD 976–1078). J Geogr Sci, 27: 606–618

He F N, Li M J, Yang F. 2019. Main progress in historical land use and land cover change in China during the past 70 years (in Chinese). J Chin Hist Geogr, 34: 5–16

He F, Li S, Zhang X, Ge Q, Dai J. 2013. Comparisons of cropland area from multiple datasets over the past 300 years in the traditional cultivated region of China. J Geogr Sci, 23: 978–990

Hou Y F. 2001. Population History of China. Vol. 6 (in Chinese). Shanghai: Fudan University Press. 97–223

Kaplan J O, Krumhardt K M, Ellis E C, Ruddiman W F, Lemmen C, Goldewijk K K. 2011. Holocene carbon emissions as a result of anthropogenic land cover change. Holocene, 21: 775–791

Kaplan J O, Krumhardt K M, Zimmermann N. 2009. The prehistoric and

preindustrial deforestation of Europe. Quat Sci Rev, 28: 3016–3034
Kaplan J, Krumhardt K, Gaillard M J, Sugita S, Trondman A K, Fyfe R, Marquer L, Mazier F, Nielsen A. 2017. Constraining the deforestation history of Europe: Evaluation of historical land use scenarios with pollen-based land cover reconstructions. Land, 6: 91
Klein Goldewijk K, Beusen A, Doelman J, Stehfest E. 2017. Anthropogenic land use estimates for the Holocene-HYDE 3.2. Earth Syst Sci Data, 9: 927–953
Klein Goldewijk K, Beusen A, Van Drecht G, De Vos M. 2011. The HYDE 3.1 spatially explicit database of human-induced global land-use change over the past 12,000 years. Glob Ecol Biogeogr, 20: 73–86
Leite C C, Costa M H, Soares-Filho B S, de Barros Viana Hissa L. 2012. Historical land use change and associated carbon emissions in Brazil from 1940 to 1995. Glob Biogeochem Cycle, 26: GB2011
Li B B, Fang X Q, Ye Y, Zhang X Z. 2010. Accuracy assessment of global historical cropland datasets based on regional reconstructed historical data—A case study in Northeast China. Sci China Earth Sci, 53: 1689–1699
Li B B, Fang X Q, Ye Y, Zhang X Z. 2014. Carbon emissions induced by cropland expansion in Northeast China during the past 300 years. Sci China Earth Sci, 57: 2259–2268
Li K, He F N, Zhang X Z. 2011. An approach to reconstructing spatial distribution of historical cropland with grid-boxes by utilizing MODIS land cover dataset: A case study of Yunnan Province in the Qing Dynasty (in Chinese). Geogr Res, 30: 2281–2288
Li M J, He F N, Li S C, Yang F. 2018b. Reconstruction of the cropland cover changes in eastern China between the 10th century and 13th century using historical documents. Sci Rep, 8: 13552
Li M J, He F N, Yang F, Li S C. 2018a. Reconstructing provincial cropland area in eastern China during the early Yuan Dynasty (AD1271–1294). J Geogr Sci, 28: 1994–2006
Li M J, He F N, Yang F, Zhao L. 2020. Reconstruction of provincial cropland area and its spatial-temporal characteristics in the Ming Dynasty (in Chinese). Geogr Res, 39: 447–460
Li M J. 2019. Reconstruction of cropland change data for eastern Asia and its spatial-temporal characteristics analysis in the last millennium (in Chinese). Doctoral Dissertation. Beijing: Institute of Geographic Sciences and Natural Resources Research, Chinese Academy of Sciences. 1–158
Li S C, He F N, Zhang X Z, Zhou T Y. 2019. Evaluation of global historical land use scenarios based on regional datasets on the Qinghai-Tibet Area. Sci Total Environ, 657: 1615–1628
Li S C, He F N, Zhang X Z. 2016. A spatially explicit reconstruction of cropland cover in China from 1661 to 1996. Reg Environ Change, 16: 417–428
Li S C, Zhang Y L, He F N. 2015. Reconstruction of cropland distribution in Qinghai and Tibet for the past one hundred years and its spatio-temporal changes (in Chinese). Prog Geogr, 34: 197–206
Lin S, Zheng J, He F. 2009. Gridding cropland data reconstruction over the agricultural region of China in 1820. J Geogr Sci, 19: 36–48
Mendelsohn R, Sohngen B. 2019. The net carbon emissions from historic land use and land use change. J Forest Econ, 34: 263–283
Nikiel C A, Eltahir E A B. 2019. Summer climate change in the Midwest and Great Plains due to agricultural development during the twentieth century. J Clim, 32: 5583–5599
Pongratz J, Reick C, Raddatz T, Claussen M. 2008. A reconstruction of global agricultural areas and land cover for the last millennium. Glob Biogeochem Cycle, 22: GB3018
Ramankutty N, Foley J A. 1999. Estimating historical changes in global land cover: Croplands from 1700 to 1992. Glob Biogeochem Cycle, 13: 997–1027
Ramankutty N. 2012. Global Cropland and Pasture Data from 1700–2007, available at: Http://www.geog.mcgill.ca/nramankutty/Datasets/Datasets.html
Scott C E, Monks S A, Spracklen D V, Arnold S R, Forster P M, Rap A, Äijälä M, Artaxo P, Carslaw K S, Chipperfield M P, Ehn M, Gilardoni S, Heikkinen L, Kulmala M, Petäjä T, Reddington C L S, Rizzo L V, Swietlicki E, Vignati E, Wilson C. 2018. Impact on short-lived climate forcers increases projected warming due to deforestation. Nat Commun, 9: 157
Stephens L, Fuller D, Boivin N, Rick T, Gauthier N, Kay A, Marwick B, Armstrong C G, Barton C M, Denham T, Douglass K, Driver J, Janz L, Roberts P, Rogers J D, Thakar H, Altaweel M, Johnson A L, Sampietro Vattuone M M, Aldenderfer M, Archila S, Artioli G, Bale M T, Beach T, Borrell F, Braje T, Buckland P I, Jiménez Cano N G, Capriles J M, Diez Castillo A, Çilingiroğlu Ç, Negus Cleary M, Conolly J, Coutros P R, Covey R A, Cremaschi M, Crowther A, Der L, di Lernia S, Doershuk J F, Doolittle W E, Edwards K J, Erlandson J M, Evans D, Fairbairn A, Faulkner P, Feinman G, Fernandes R, Fitzpatrick S M, Fyfe R, Garcea E, Goldstein S, Goodman R C, Dalpoim Guedes J, Herrmann J, Hiscock P, Hommel P, Horsburgh K A, Hritz C, Ives J W, Junno A, Kahn J G, Kaufman B, Kearns C, Kidder T R, Lanoë F, Lawrence D, Lee G A, Levin M J, Lindskoug H B, López-Sáez J A, Macrae S, Marchant R, Marston J M, McClure S, McCoy M D, Miller A V, Morrison M, Motuzaite Matuzeviciute G, Müller J, Nayak A, Noerwidi S, Peres T M, Peterson C E, Proctor L, Randall A R, Renette S, Robbins Schug G, Ryzewski K, Saini R, Scheinsohn V, Schmidt P, Sebillaud P, Seitsonen O, Simpson I A, Sołtysiak A, Speakman R J, Spengler R N, Steffen M L, Storozum M J, Strickland K M, Thompson J, Thurston T L, Ulm S, Ustunkaya M C, Welker M H, West C, Williams P R, Wright D K, Wright N, Zahir M, Zerboni A, Beaudoin E, Munevar Garcia S, Powell J, Thornton A, Kaplan J O, Gaillard M J, Klein Goldewijk K, Ellis E. 2019. Archaeological assessment reveals Earth's early transformation through land use. Science, 365: 897–902
Tan Q X. 1982. The Historical Atlas of China (in Chinese). Beijing: SinoMaps Press
Tian H Q, Banger K, Bo T, Dadhwal V K. 2014. History of land use in India during 1880–2010: Large-scale land transformations reconstructed from satellite data and historical archives. Glob Planet Change, 121: 78–88
Verburg P H, Crossman N, Ellis E C, Heinimann A, Hostert P, Mertz O, Nagendra H, Sikor T, Erb K H, Golubiewski N, Grau R, Grove M, Konaté S, Meyfroidt P, Parker D C, Chowdhury R R, Shibata H, Thomson A, Zhen L. 2015. Land system science and sustainable development of the earth system: A global land project perspective. Anthropocene, 12: 29–41
Wang Y H. 1980. Some experiences and lessons of historical land use in China (in Chinese). Agric Sci China, 1: 90–96
Wu S D. 2000. Population History of China. Vol. 3 (in Chinese). Shanghai: Fudan University Press. 418–570
Wu Z L, Fang X Q, Jia D, Zhao W Y. 2020. Reconstruction of cropland cover using historical literature and settlement relics in farming areas of Shangjing Dao during the Liao Dynasty, China, around 1100 AD. Holocene, 30: 1516–1527
Yang X H, Jin X B, Guo B B, Long Y, Zhou Y K. 2015. Research on reconstructing spatial distribution of historical cropland over 300years in traditional cultivated regions of China. Glob Planet Change, 128: 90–102
Yang X, Jin X, Xiang X, Fan Y, Liu J, Shan W, Zhou Y. 2019. Carbon emissions induced by farmland expansion in China during the past 300 years. Sci China Earth Sci, 62: 423–437
Yang X H, Xue Q F, Zhou Y K. 2021. Reconstruction of farmland dataset of Taiwan province in recent 300 years (in Chinese). J Nat Reso, 36: 2163–2178
Ye Y, Fang X Q, Ren Y Y, Zhang X Z, Chen L. 2009. Cropland cover change in Northeast China during the past 300 years. Sci China Ser D-Earth Sci, 52: 1172–1182
Yu S S, Zhang Z X, Liu F, Wang X, Hu S G. 2019. Assessing interannual urbanization of China's six megacities since 2000. Remote Sens, 11: 2138
Zhang A F. 2017. The Study on the Economy of Western Region Reclamation and Xinjiang Development (in Chinese). Guangzhou: Guangdong People's Press
Zhang C P. 2020. Development of a gridded allocation algorithm of his-

torical cropland derived from the physiogeographic factors—A case study of China (in Chinese). Doctoral Dissertation. Beijing: Beijing Normal University. 1–155
Zhang D Y, Fang X Q, Yang L E. 2021. Comparison of the HYDE cropland data over the past millennium with regional historical evidence from Germany. Reg Environ Change, 21: 15
Zhang P Y. 1996. Historical Climate Change in China (in Chinese). Jinan: Shangdong Science and Technology Press. 403–406
Zhao Y Z. 2010. Study on Reclamation of the Silk Road (in Chinese). Urumqi: Xinjiang People's Press. 115–210
Zou Y L. 1995. The shift of the northern farming-pastoral transitional zone and the change of cold and warm climate in the Ming and Qing dynasties (in Chinese). J Fudan Univ-Soc Sci, 1: 25–33
Zumkehr A, Campbell J E. 2013. Historical U.S. cropland areas and the potential for bioenergy production on abandoned croplands. Environ Sci Technol, 47: 3840–3847

(Responsible editor: Jianhui CHEN)